2021

Development of State-of-the-art Experimental Technique to Investigate Temperature Field in Leakage Flows of Positive Displacement Machines

Brijeshkumar Patel
City, University of London, brijeshkumar.patel@city.ac.uk

Ahmed Kovacevic
City, University of London

Md nahinul Alam
City, University of London

Alexandros Charogiannis
LavisionUK Ltd.

Development of state-of-the-art experimental technique to investigate temperature field in leakage flows of positive displacement machines

Brijeshkumar PATEL[1]*, Ahmed KOVACEVIC[2], Md Nahinul ALAM[3], Alexandros CHAROGIANNIS[4]

[1,2,3] City, University of London, London, UK, EC1V0HB

[4] LavisionUK Ltd, United Kingdom

[1]Brijeshkumar.patel@city.ac.uk
[2]A.Kovacevic@city.ac.uk
[3]Md.Alam.5@city.ac.uk
[4]ACharogiannis@lavision.com

* Corresponding Author

ABSTRACT

Investigation of leakage flows in oil-free rotary positive displacement machines (PDMs) is necessary to get a real insight into attributes of leakage flows. Experimental study of heat transfer in the leakage flows of the oil-free positive displacement machines is challenging. The primary reason is complexities associated with actual machine running condition such as extremely small (micron-size) clearance gap, high speed of rotors, optical access of flows etc. Therefore, this study presents the development of state-of-the-art experimental setup using Planar Laser-Induced Fluorescence (PLIF) technique to visualize the temperature field in the clearance flows of rotary machines. This study considers Roots blower to implement PLIF technique because it provides relatively easy optical access. Besides, it is a good representative of PDMs. Selection criteria of optical glass, suitable tracer particles, Imaging camera, optical lenses and filters are investigated in detail. Pixel Intensity was found to be conformable in the clearance gap from recorded images of temperature field, thereby confirmed the efficacy of the flow visualization and instrumentation systems developed.

1. INTRODUCTION

Rotary machines are present in the majority of energy generation and conversion systems. Today's compressed air sector utilizes almost 20% of a world generated power, which is why these machines contribute highly in carbon emission(Vittorini et al., 2015). So, this study focuses explicitly on oil-free rotary machines. As depicted in Figure 1, all rotary machines have a clearance gap to allow motion between stator and rotor, and these clearance gaps are one of the significant contributors to efficiency loss. Nowadays, it is possible to maintain optimal clearance gap in rotary machines, but it introduces question on the reliability of machines as clearance gap size varies in running condition.

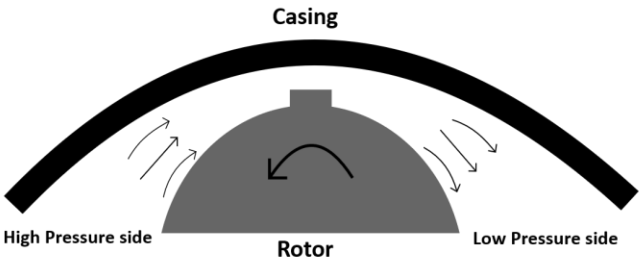

Figure 1 Leakage through the gap between casing and rotor

As per the literature on leakage flows, flow dynamics within the clearance gap is present(Coull & Atkins, 2015; Kauder & Stratmann, 2002; Sachs, 2002). These flow dynamics are greatly affected by the pressure difference

across the gap and gap size, at higher pressure ratios flow separation and shocks are observed. Shock boundary layer and shearing directly affect the heat transfer rates, and these variable heat transfer can lead to uneven material growth in the machine's actual running condition (Zhang et al., 2011). Therefore, knowledge of heat transfer inside the clearance gap is vital. Experimental study of the temperature field to get an insight of the clearance gap is necessary but challenging because of the tiny micron size gap and high speed of rotors. In the present study, an oil-free Roots blower is considered as a representative of positive displacement machines because it provides comparatively easy optical access.

Recently, many researchers have used PLIF to study multiphase flows as well as organic constituents and quantitative analysis(Charogiannis et al., 2019; Richardson et al., 2017). Few of them have focused on an application of LIF for the study of temperature field in combustion engines and multiphase flows(Charogiannis & Markides, 2019; Kranz et al., 2018; Rothamer et al., 2009). The same technique can be utilized to study the temperature field in the clearance of rotary positive displacement machine. However, due to the very small size of the clearance gap and rotation of the machine, it is hard to implement a setup used by the researcher in the past. Therefore, this study focuses on developing a unique experimental setup using PLIF technique to obtain temperature field in the clearance gap of roots blower. The detailed procedure of selection of optical glass, tracer particles for LIF, optical instruments are explained.

2. EXPERIMENTAL MODELING APPROCH

2.1. Theoretical background of PLIF

The LIF technique allows for spatiotemporally-resolved, non-intrusive measurements of scalar fields such as temperature and species concentration by quantitatively interpreting the light emitted by a tracer molecule. In greater detail, upon excitation by a light/laser source, tracer molecules gain energy which is sometimes dissipated by photon emission. These photons are collected by a camera and the resulting signal is quantified according to its dependencies on any relevant flow parameters. The quantification of these dependences necessitates an in-depth understanding of the physics underlying the excitation and deexcitation of the employed molecular tracer and a calibration.

The total collected LIF (S_{LIF}) signal can be described by the following relationship,

$$S_{LIF} = \eta_{opt}\left(\frac{E_{pulse}\,\lambda}{Ahc}\right) V_{pix} \nu_{tracer} \sigma_{abs} \phi_f \tag{1}$$

Where η_{opt} stands for the efficiency of the collection optics and incorporates factors such as the solid angle of the detector lens and the spectral responsivity of the detection system. E_{Pulse} is local laser fluence, h is plank constant, c is speed of light in vacuum, λ is wavelength and A is laser sheet area. Altogether the bracketed term represents the number of excitation photons per laser-sheet cross-sectional area. The product of the size of the imaged volume (V_{pix}) along the laser sheet propagation times the tracer number density (ν_{tracer}) gives the number of tracer molecules available for excitation. The last two terms, the absorption cross-section (σ_{abs}) and the fluorescence quantum yield (φ_f) account for the photophysical dependencies of the fluorescence signal and represent the probability of absorption and the efficiency of fluorescence emission respectively.

The two-colour detection approach (2-colour LIF) requires the illumination of the seeded volume and the subsequent detection of the emitted fluorescence by two detectors simultaneously (each looking at a different part of the emission spectrum). The resulting signal ratio (here abbreviated as $S_{\lambda 1}/S_{\lambda 2}$) depends only on the absorption cross-section and the fluorescence quantum yield of the tracer at the respective wavelength ranges(Rothamer et al., 2009), as dependencies such as the pulse-to-pulse energy variation and tracer density cancel out, while others such as the efficiency of the detection optics are incorporated in a constant (C).

$$\frac{S_{\lambda 1}}{S_{\lambda 2}} = C\,\frac{\sigma_{abs}\varphi_{f_{\lambda 1}}}{\sigma_{abs}\varphi_{\lambda 2}} = f\left(T, \upsilon_{o_2}\right) \tag{2}$$

In this experimental method, the fluid flow area of interest is illuminated by a laser sheet. The resulting fluorescence light from excited molecules in the light sheet is imaged through a selective filter onto a time-gated digital camera. For pulsed UV LIF applications usually, an image intensifier amplifies the LIF signal. The conversion of LIF images into a meaningful concentration or temperature fields is based on calibration measurements.

2.2. Optical roots blower

In this study, Roots blower URAI-22 from Howden is used. Optical access is required on the Roots blower to visualize the temperature field in the clearances. To get optical access of radial leakage path some portion (Area bounded by the yellow line in Figure 2) of the Roots blower is replaced by optical material. For the current application, optical material should be able to withstand high temperature and pressure up to 300 °C and 7 barg respectively. Besides, specifically for PLIF technique, the optical element should be transparent for UV light.

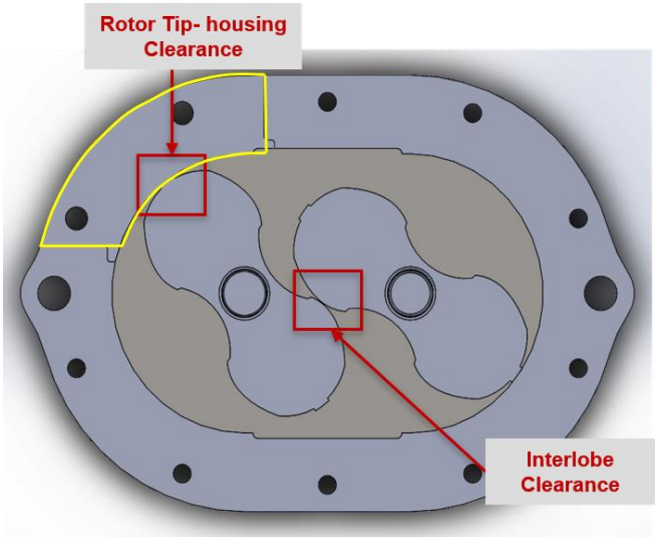

Figure 2 Clearances in Roots blower

For optical access, fused silica glass is the best suitable material for our application. Figure 3 (a) shows a complex shape of the optical Glass manufactured from the Fused silica. As shown in Figure 3 (b) & (c), Optical access from radial direction and side of the Roots blower is provided to visualize a flow in clearance gap between rotor tip and housing. A thin gasket is used between metal and Glass surface to avoid any direct contact to reduce risk of cracking in the Glass at higher working temperature. Glass is kept tight using an external metal plate to eliminate leakage through glass and metal mating surfaces.

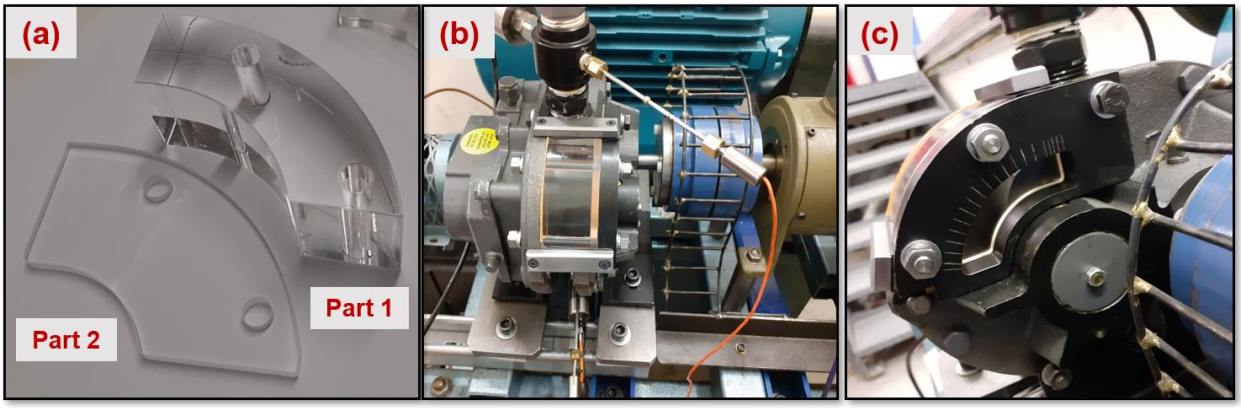

Figure 3 (a) Optical element from Fused silica Glass (b) Radial optical access of Roots blower (c) optical access from side of Roots blower

2.3. PLIF test setup

The layout of the Roots blower test rig is depicted in Figure 4. Roots blower is connected with variable speed electric motor through pulley transmission system to run at various operating condition, and Roots blower can run up to 2700 RPM based on current pulley ratio. To monitor and control the operating parameter of the machine, pressure and temperature sensors are installed at suction (P1, T1), discharge (P2, T2) and Orifice (ΔP, T3). Shaft encoder and torque meter are used to measure the speed and power of roots blower. The flow of the machine measures using Orifice. The ball valve is installed in the discharge line of the machine require discharge pressure. By partially closing the valve, we can increase the discharge pressure of the machine. All sensors are connected with National instrument-based data acquisition system, and real-time data are recorded using LabView based programming.

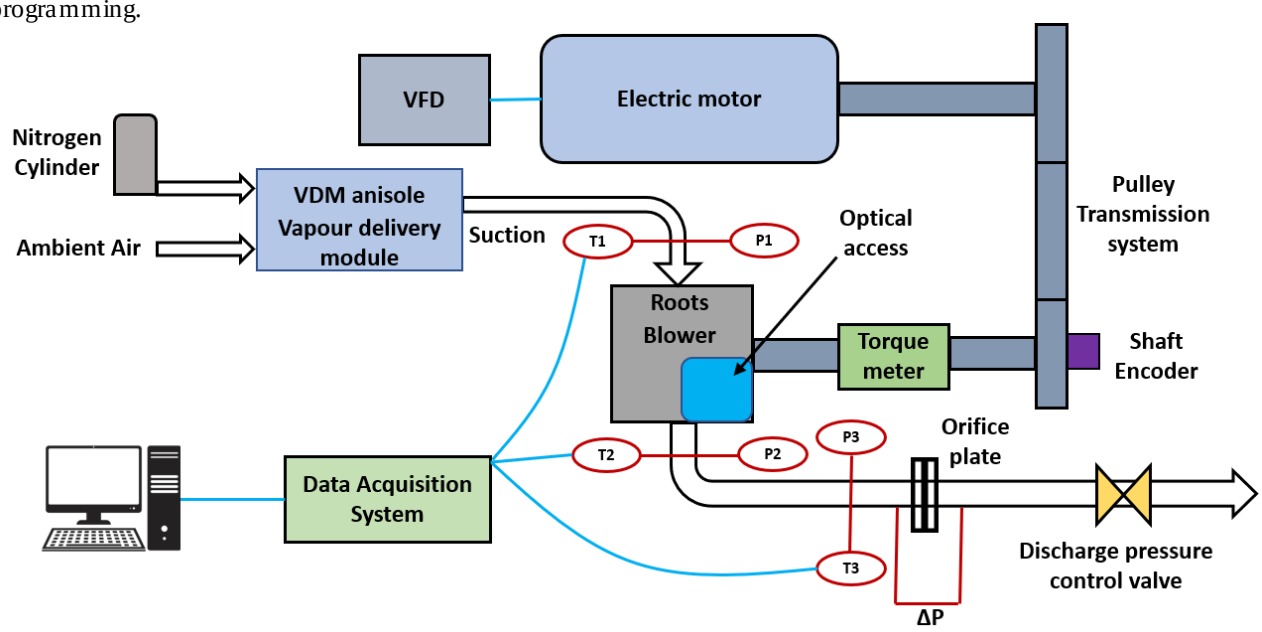

Figure 4 Layout of the Roots blower test rig

Detailed arrangement of optical access of Roots blower with laser is shown in Figure 5. The beam from a Q-smart QSM-850 Nd: YAG laser at 1064 nm is guided through 2ω and 4ω module to convert it into 266nm. A combination of optical sheet and – 50mm cylindrical lens then form a laser sheet. The sheet had a thickness of about 1mm, and it was placed at the central plane of lobes of roots blower passing through curved fused silica window. The average laser shot energy in the observation area was 100 mJ. Owing to spatial constraints, the emitted fluorescence light was rotated by 90°using a UV mirror and guided to the detection optics. Two filters, 320nm with 40nm bandwidth and 280nm with 20nm bandwidth are used. Filters with 320nm and 280nm are determined based on the fluorescence spectra obtain by Faust(Faust et al., 2014). It is necessary to change the filters alternatively at each measuring condition to capture the images with a single camera. One CMOS camera with LaVision intensified relay optics (IRO) with UV camera lenses (LaVision, f = 100 mm, f/2.8) image the field of view. Phase-locked at a particular crank angle is achieved by LaVision external triggering device with custom signal modulation. At each crack angle, 200 consecutive images are captured.

Following the two-colour strategy for measuring the temperature, the anisole fluorescence is seeded using a Bronkhorst anisole seeder. Here we choose anisole as a seeding fluorescence particle because it yields the best signal per volume in both Nitrogen and air(Faust et al., 2014). The carrier gas was Nitrogen, and the flowrate of anisole and nitrogen mixture could be adjusted using a mass flow controller of VDM vapour delivery module. For most experiments, this was kept about 5 LPM. Different flow rates are supplied at the beginning of experiment and intensity values in the captured images were checked to get the sufficient optimum flow rate value of anisole. The output of the seeder was introduced at the suction hose of the Roots blower.

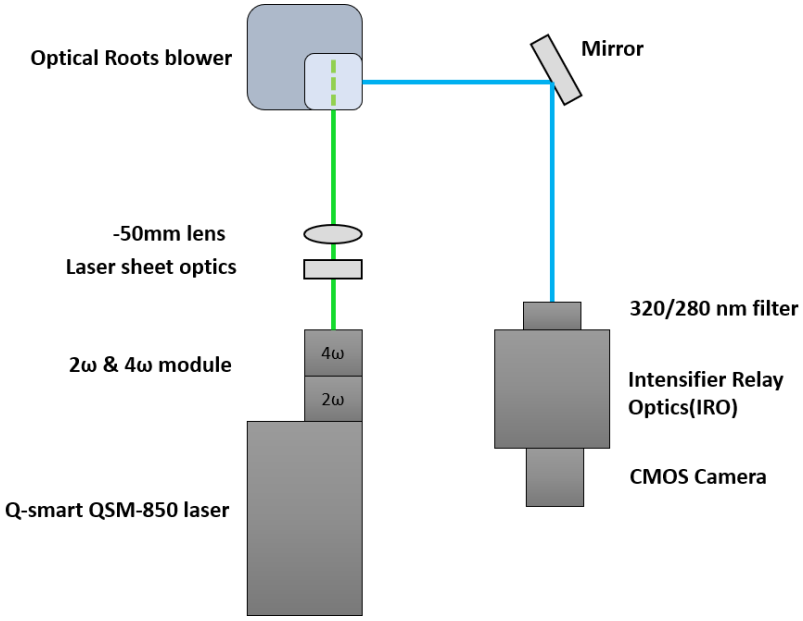

Figure 5 Layout of optical instrument arrangement for PLIF imaging

The final arrangement of PLIF optics with Roots blower test rig is shown in Figure 6, including laser, laser arm, camera, UV optics, roots blower test rig, Seeder and two sperate DAQ system. One DAQ is used to operate roots blower test rig, and another is used to operate the imaging process.

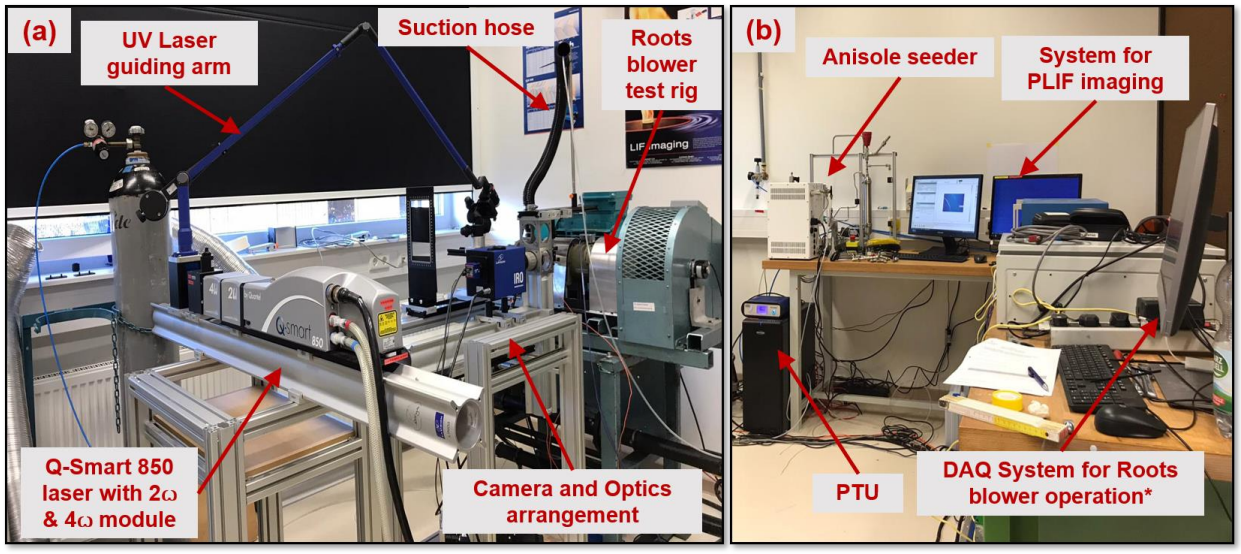

Figure 6 (a) Arrangement of PLIF optics (b) DAQ system for blower operation and PLIF imaging

3. RESULTS AND DISCUSSION

Using the experimental setup as described in the previous section, LIF images are recorded in the running condition of the machine. For particular crank angle (here 50°) of the rotor, total 200 consecutive images are recorded using 320nm and 280nm filters. The average intensity of illuminated fluorescence particles in the clearance at running speed of 300RPM and 22° C discharge temperature is shown in Figure 7. Location of clearance gap at the tip of the rotor is highlighted in Figure 7. Flow field above clearance is on the suction side while flow field below clearance is on the discharge side.

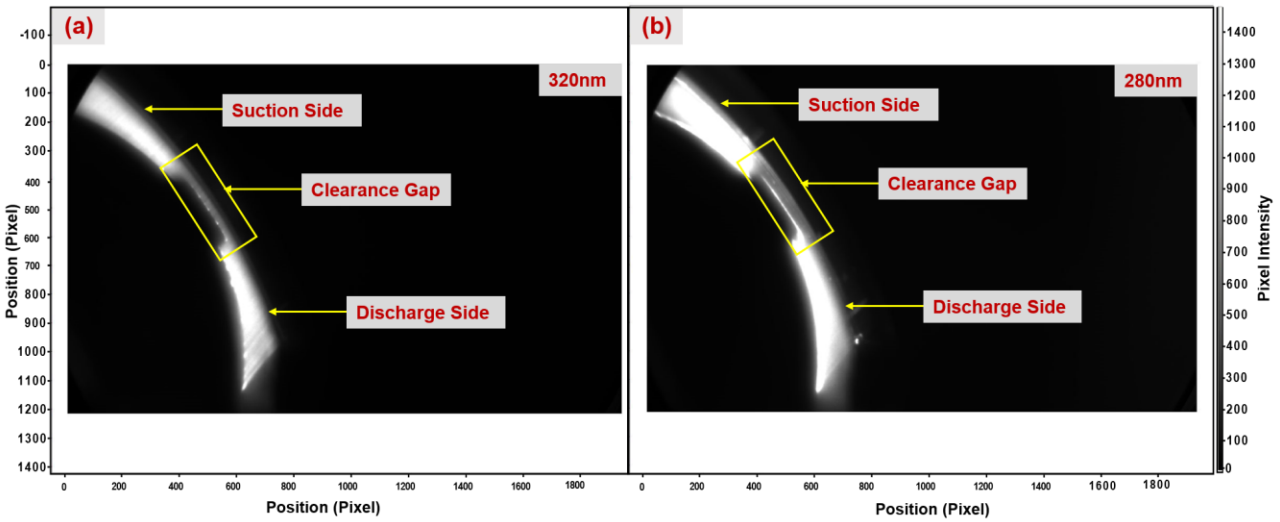

Figure 7 (a) Image captured by 320nm filter at 300 RPM (b) Image captured by 280nm filter at 300 RPM

In order to obtain the temperature from these recorded images, according to equation (2) ratio of images with 320nm and 280nm is needed, Image ratio is presented in Figure 8. Pixel values of image ratio represent the ratio of intensity which is the function of temperature. The stringent calibration process is needed to convert pixel values into temperature. Calibration is not a part of the present study, however it is assumed that measured discharge temperature by RTD is equal to temperature in discharge pocket (Discharge end in Figure 7and Figure 8) to compare the pixel intensity and determine acceptable level of intensity value. Image ratio presents reasonable intensity inside the clearance gap, which shows the capability of developed setup to get the temperature in the clearance gap of the rotary machine in running condition. However, some portion of reflection is observed on the suction side (Figure 8). Besides, few high-intensity spots are observed on the surface of the rotor; those are the noise in the captured images. Probable causes of these spots are black paint of the rotor surface and high energy of the laser. To check the quality of images, tests were also run at higher speed of 600, 900,1200 and 1500. Images found to be good except some reflection on suction side.

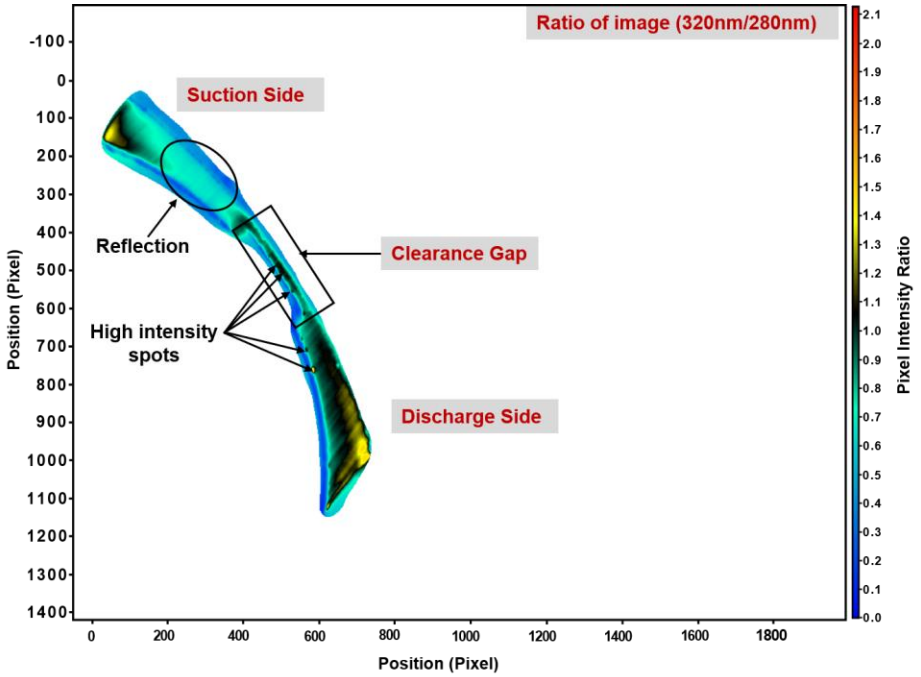

Figure 8 Image ratio (320nm/280nm) at 300 RPM

4. CONCLUSIONS

In summary, this study focuses on the application of PLIF to get temperature field in the Clearance gap of rotary machines by using a developed experimental setup. Images recorded with two different filters and image ratios obtained from those images represent an acceptable range of pixel values to produce a temperature field. Minor flaws are observed, like reflection and high-intensity spots, which can create little difficulty in getting the accurate temperature in the suction area and on the surface of the rotor. Still, these flaws can be addressed in future work. Therefore, a developed setup using the LIF technique is able to produce a reasonable temperature field in the clearance gap. This setup is helpful to reveal the physics of heat transfer in the clearance gap of the oil-free positive displacement machines.

NOMENCLATURE

A	Laser sheet area	(m^2)
C	Constant	(–)
c	Speed of light	(m/s)
E	Laser energy	(mJ)
h	Plank constant	(Js)
P	Pressure	(Bara)
S	Signal	(–)
T	Temperature	(k)
V	Imaged Volume	(m^3)
υ	Number of pixels per unit area (Tracer density)	(–)
η	Efficiency	(–)
σ	Cross section of area under investigation	(–)
φ	Quantum yield	(–)
λ	wavelength	(nm)

Subscript

LIF	Laser Induced fluorescence
opt	Optics
pulse	Laser pulse
pix	Pixel of image
abs	Absorption
f	Fluorescence

REFERENCES

Charogiannis, A., & Markides, C. N. (2019). Spatiotemporally resolved heat transfer measurements in falling liquid-films by simultaneous application of planar laser-induced fluorescence (PLIF), particle tracking velocimetry (PTV) and infrared (IR) thermography. *Experimental Thermal and Fluid Science*, *107*, 169–191. https://doi.org/10.1016/j.expthermflusci.2018.11.001

Charogiannis, A., Sik An, J., Voulgaropoulos, V., & Markides, C. N. (2019). Structured planar laser-induced fluorescence (S-PLIF) for the accurate identification of interfaces in multiphase flows. *International Journal of Multiphase Flow*, *118*, 193–204. https://doi.org/10.1016/j.ijmultiphaseflow.2019.06.002

Coull, J. D., & Atkins, N. R. (2015). *The Influence of Boundary Conditions on Tip Leakage Flow*. *137*(June), 1–10. https://doi.org/10.1115/1.4028796

Faust, S., Goschütz, M., Kaiser, S. A., Dreier, T., & Schulz, C. (2014). A comparison of selected organic tracers for quantitative scalar imaging in the gas phase via laser-induced fluorescence. *Applied Physics B: Lasers and Optics*, *117*(1), 183–194.

https://doi.org/10.1007/s00340-014-5818-x

Kauder, P. K., & Stratmann, D. D. (2002). *Theoretical Gas Flow through Gaps in Screw-type Machines*.

Kranz, P., Fuhrmann, D., Goschütz, M., Kaiser, S., Bauke, S., Golibrzuch, K., Wackerbarth, H., Kawelke, P., Luciani, J., Beckmann, L., Zachow, J., Schuette, M., Thiele, O., & Berg, T. (2018). In-Cylinder LIF Imaging, IR-Absorption Point Measurements, and a CFD Simulation to Evaluate Mixture Formation in a CNG-Fueled Engine. *SAE International Journal of Engines*, *11*(6), 1221–1238. https://doi.org/10.4271/2018-01-0633

Richardson, D. R., Roy, S., & Gord, J. R. (2017). Femtosecond, two-photon, planar laser-induced fluorescence of carbon monoxide in flames. *Optics Letters*, *42*(4), 875. https://doi.org/10.1364/ol.42.000875

Rothamer, D. A., Snyder, J. A., Hanson, R. K., & Steeper, R. R. (2009). Two-wavelength PLIF diagnostic for temperature and composition. *SAE International Journal of Fuels and Lubricants*, *1*(1), 520–533. https://doi.org/10.4271/2008-01-1067

Sachs, R. (2002). *Experimental investigation of Gas flows in screw machines*.

Vittorini, D., Bianchi, G., & Cipollone, R. (2015). Energy saving potential in existing volumetric rotary compressors. *Energy Procedia*, *81*, 1121–1130. https://doi.org/10.1016/j.egypro.2015.12.137

Zhang, Q., O'Dowd, D. O., He, L., Wheeler, A. P. S., Ligrani, P. M., & Cheong, B. C. Y. (2011). Overtip shock wave structure and its impact on turbine blade tip heat transfer. *Journal of Turbomachinery*, *133*(4), 1–8. https://doi.org/10.1115/1.4002949